Abdominal Radiology (2019) 44:3139–3147
https://doi.org/10.1007/s00261-019-02084-2

PANCREAS

Invasive intraductal papillary mucinous neoplasms of the pancreas: relationships between mural nodules detected on thin-section contrast-enhanced MDCT and invasive components

Noritaka Kamei[1] · Yasunari Yamada[1] · Naoki Hijiya[2] · Ryo Takaji[1] · Maki Kiyonaga[1] · Norio Hongo[1] · Masayuki Ohta[3] · Teijiro Hirashita[3] · Masafumi Inomata[3] · Shunro Matsumoto[1]

Published online: 5 June 2019

Abstract

Purpose To elucidate the relationships between mural nodules (MNs) and invasive components in patients with invasive intraductal papillary mucinous neoplasm (IPMN) on the basis of thin-section contrast-enhanced multidetector CT (CE-MDCT) and pathologic findings.

Methods This retrospective study included 28 patients with surgically confirmed invasive IPMN. Two radiologists independently evaluated the thin-section (1-mm section thickness, no overlap) triple-phase CE-MDCT images for MNs, invasive components, and the continuity between them using a five-point scale (confidence scores of 1–3 as negative, 4 and 5 as positive). Kappa statistic was used to evaluate interobserver agreement. The CE-MDCT findings were correlated with pathologic findings.

Results Interobserver agreement was good or excellent. MNs consisting of tumor cells were recognized in 12 (42.9%) of 28 patients with no discrepancy between the two radiologists. Invasive components were detected in 85.7% and 82.1% in the pancreatic parenchymal phase for radiologist 1 and 2, respectively, and recognized as hypoattenuating areas. Pathologic continuities between MNs and invasive components were confirmed in five (41.7%) of 12 patients with MNs and these were detected on CE-MDCT. When combined seven patients without continuities between MNs and invasive components and 16 patients without MNs, the invasive components pathologically derived from non-nodular low-height papillary epithelium in 23 (82.1%) of 28 patients.

Conclusions The invasive components derived more often from low-height papillary epithelium without MN appearance on CE-MDCT than from MN. Careful attention should be paid to the existence of an invasive component even in the absence of an enhancing MN.

Keywords Pancreatic neoplasms · Multidetector computed tomography · Pancreatic ducts

Abbreviations

EUS	Endoscopic ultrasonography
MDCT	Multidetector computed tomography
CE	Contrast enhanced
IPMN	Intraductal papillary mucinous neoplasm
MN	Mural nodule
MPD	Main pancreatic duct

Introduction

Intraductal papillary mucinous neoplasms (IPMNs) have the potential to progress from low-grade dysplasia to invasive carcinoma over the time [1–3]. The overall 5-year survival rates after surgery for malignant IPMNs are 92.0−96.2% in non-invasive (high-grade dysplasia) IPMNs, 79−81.0% in minimally invasive IPMNs (invasive depth ≤ 5.0 mm), and 38−59.0% in invasive IPMNs (invasive depth > 5.0 mm) [4–7]. It is well established that imaging findings, including dilatation of the main pancreatic duct (MPD) and branch

✉ Yasunari Yamada
yasunari@oita-u.ac.jp

[1] Department of Radiology, Oita University Faculty of Medicine, 1-1 Hasama-machi, Yufu, Oita 879-5593, Japan

[2] Department of Molecular Pathology, Oita University Faculty of Medicine, Yufu, Oita 879-5593, Japan

[3] Department of Gastrointestinal and Pediatric Surgery, Oita University Faculty of Medicine, Yufu, Oita 879-5593, Japan

ducts, mural nodules (MNs), and a thickened cyst wall are associated with malignancy, and an enhancing MN is considered to be the most significant risk factor [8–12]. It has been previously reported that MNs ≥ 5−10 mm carry a high risk of malignancy [10, 12, 13] and that high-grade dysplasia is located within MNs in 70−90% of malignant IPMN cases [13, 14]. This led us to a hypothesis that the invasive components would derive from MNs with high-grade dysplasia in patients with invasive IPMN. Elucidation of the prevalence of MNs, the location of the invasive components, and the presence or absence of continuity between MNs and the invasive components may be necessary to diagnose early-stage invasive IPMN with imaging. To our knowledge, there have been no reports that have evaluated these relationships between the MNs and invasive components on imaging in patients with invasive IPMN. Computed tomography (CT) examination has similar diagnostic performance compared to magnetic resonance imaging (MRI) and endoscopic ultrasound (EUS) for evaluating patients with IPMN [15–17]. CT is one of the diagnostic modalities which are recommended for evaluation of the IPMN in the International Association of Pancreatology consensus guidelines [8, 11] and is recommended by the European Study Group on Cystic Tumors of the Pancreas 2018 guidelines [12] when there is suspicion of malignant IPMN.

The purpose of our study is to elucidate the relationships between MNs and invasive components in patients with invasive IPMN on the basis of thin-section contrast-enhanced multidetector CT (CE-MDCT) and pathologic findings.

Materials and methods

Study population

This retrospective study was approved by the Institutional Review Board, and the requirement for informed consent was waived. Between June 2008 and December 2017, all consecutive patients who were known or suspected to have pancreatic or biliary tract disease underwent a thin-section triple-phase CE-MDCT examination at our institution. Suspected IPMNs of the pancreas underwent surgical resection after findings suspicious for malignancy were identified, including the diameter of dilated branch ducts and MPD, the presence of MN and/or invasive components, and obstructive jaundice according to previous reports [18–20], and guidelines for the management of IPMN [8, 11]. By reviewing the surgical records of the patients, 31 consecutive patients were identified, meeting the following inclusion criteria: the tumor was surgically resected and the diagnosis of invasive IPMN was pathologically confirmed. Three patients were excluded because of having a history of renal failure ($n = 1$) and a contraindication to iodinated contrast material ($n = 2$). The study group, therefore, comprised 28 patients (14 men and 14 women; mean age, 70.9 years; range, 55–85 years).

Surgical procedures and pathologic sections

Lesions were resected using pylorus-preserving pancreatoduodenectomy in nine patients, pancreatoduodenectomy in eight patients, distal pancreatectomy in ten patients, and total pancreatectomy in one patient. The resected specimens were cut stepwise into 5 mm sections perpendicular to the MPD, fixed in a 10% formaldehyde solution and stained with haematoxylin–eosin and examined under a light microscope. Pathologic evaluation was performed by an experienced pathologist (N.H.) with 29 years of experience.

CT protocols and contrast materials

Non-contrast and triple-phase CE-MDCT is usually performed with thin-section scanning (1-mm section thickness, no overlap) in cases of suspected pancreatic lesions [21–23]. Pancreatic parenchymal (determined by using a bolus-triggering method), portal venous (70 s), and equilibrium phases (155 s) were acquired in all patients after the intravenous injection of 100 mL contrast medium (Iopamiron 370®, Bayer Schering Pharma, Berlin, Germany) at a rate of 3 mL/s using a power injector. Technical details are provided in Table 1. The data sets obtained were sent to a computer workstation (Aquarius NetStation Version 1.2®, TeraRecon, San Mateo, CA, USA). Image analysis was performed on axial and parasagittal reconstruction images perpendicular to the MPD similar to the pathologic sections. The mean interval between the preoperative CE-MDCT scan and the surgical resection was 16.3 ± 7.6 days (range 4–29 days).

Detection of MNs on CE-MDCT and pathologic correlation in patients with invasive IPMN

Two radiologists (N.K. and Y.Y. with 16 and 29 years of experience in abdominal imaging, respectively) independently assessed the MNs on triple-phase CE-MDCT images in 28 patients with invasive IPMN. An MN was defined as a well-circumscribed enhancing structure in the MPD and/or branch ducts. The radiologists were aware of the diagnosis of IPMN, but they were blinded to other preoperative images such as MRI and EUS and the details regarding the pathologic findings (e.g., low-grade dysplasia, high-grade dysplasia, and invasive carcinoma), as well as any clinical or laboratory information. The two radiologists rated the confidence level of their assessment of the presence of MNs using a 5-point scale (1: definitely not seen; 2: probably not seen; 3: equivocal; 4: probably seen; 5: definitely seen). Any discrepancies were resolved during a third-analysis session,

Table 1 Protocols of the thin-section triple-phase contrast-enhanced multidetector CT

Parameter		
Scanner	Aquilion CX TSX-101A/NA or ONE TSX-301A/2A	Aquilion ONE First Genesis TSX-305A/1 W
Helical pitch	0.84	0.81
Rotation time (s)	0.5	0.5
Beam collimation (mm)	32	20
No. of detector rows	CX TSX-101A/NA: 64	320
Ffed	ONE TSX-301A/2A: 320	
Detector configuration	1.0×32	0.5×40
Scan field of view	400	500
kV	120	120
Smart mA min/max mA range	10/500	10/600
Noise index	11	12
Reconstruction (filtered back projection)		
Display field of view (cm)	35	35
Reconstruction type	FC14	FC14
Slice thickness (mm)	1.0	1.0
Slice interval (mm)	1.0	1.0
Window width/level (Hounsfield unit)	300/10 (unenhanced image)	300/10 (unenhanced image)
	350/40 (contrast-enhanced image)	350/40 (contrast-enhanced image)

in which a decision was reached by consensus between the two radiologists. The confidence level ratings of 1−3 were defined as negative detection, and those of 4 and 5 as positive detection. The MNs detected on CE-MDCT were correlated with the pathologic findings. For the MNs that were pathologically proven papillary tumor epithelium, the histologic type (low-grade dysplasia or high-grade dysplasia), site of origin (MPD and/or branch duct), and maximum diameters of the MNs on the pathologic specimens were recorded. The maximum diameters of MNs, MPDs, and dilated branch ducts were measured on CE-MDCT in each patient by two radiologists in consensus.

Qualitative evaluation of invasive components on CE-MDCT based on pathologic findings in patients with invasive IPMN

Invasive components were qualitatively assessed in the triple-phase CE-MDCT images in 28 patients and defined as a hypo- or hyperattenuating area in the pancreatic parenchyma contiguous with dilated pancreatic ducts. CE-MDCT images were independently reviewed by two radiologists (N.K. and Y.Y.). The CE-MDCT images of each phase in all patients were divided into three groups in random fashion to prevent the different phase images of the same patients from being the same group. The review of each group of images was performed with an interval of at least 1 month to minimize learning bias, and the images were presented in random order. Two radiologists rated the confidence level of their assessment of the presence of the invasive component using a 5-point scale (1: definitely not seen; 2: probably not seen; 3: equivocal; 4: probably seen; 5: definitely seen). The confidence level ratings of 1–3 were defined as negative detection, and those of 4 and 5 as positive detection. The invasive components and surrounding pancreatic parenchyma were correlated with pathologic findings. The invasive components were classified by histologic type (tubular or mucinous adenocarcinoma) and the maximum diameter of the invasive component was measured on the pathologic specimens. The sites of origin (MPD and/or branch duct) of the invasive components were investigated.

Relationships between MNs and the invasive components on the basis of CE-MDCT and pathologic findings

In patients with MNs, the continuity between MNs and invasive components, namely, the transition from the high-grade dysplasia within the MNs to the invasive components, was pathologically assessed. In patients with ≥2 MNs, the continuities between all MNs and invasive components were assessed. Two radiologists (N.K. and Y.Y.) independently assessed the continuity between MNs and invasive components on CE-MDCT. The two radiologists rated the confidence level of their assessment of the presence of the continuity using a 5-point scale (1: definitely not seen; 2: probably not seen; 3: equivocal; 4: probably seen; 5: definitely seen). The confidence level ratings of 1-3 were defined

as negative continuity, and those of 4 and 5 as positive continuity. Morphologic classification of invasive IPMNs was performed on the basis of the relationships between MNs and invasive components in the pathologic findings. In patients with continuity between MN and invasive component, the location (branch duct or MPD) of the continuity was evaluated. In patients without the continuity, the location of each MN and invasive component was evaluated. In patients without MNs, the location of the invasive component was evaluated.

Data analysis

Interobserver agreement in the detection of MN, the invasive component, and continuity between the two on CE-MDCT was evaluated using the linear-weighted κ statistic: value of 0.21–0.40 indicated poor agreement; 0.41–0.60, fair agreement; 0.61–0.80, good agreement; and 0.81–1.00, excellent agreement [24]. Student *t* test (for normally distributed data) or Mann–Whitney *U* test (for non-normally distributed data) was used to compare the mean diameter of the MN between CE-MDCT images and the pathologic specimens; the mean diameter of the MPDs, dilated branch ducts, and invasive components between patients with and without MN; the mean diameter of the MNs between patients with and without continuity between MN and the invasive component. All analyses were conducted using a software excel statistics (SPSS version 15.0; SPSS Inc., Chicago IL, USA). A p value of <0.05 was considered to indicate a significant difference.

Results

Detection of MNs on CE-MDCT and pathologic correlation in patients with invasive IPMN

A 5-point scale assessment of the presence of MNs on CE-MDCT revealed excellent agreement between the two radiologists with weighted κ statistics of 0.90 (95% confidence interval [CI] 0.82, 0.98). For each radiologist, MNs were detected in 14 of 28 patients and two MNs were detected in one patient. No discrepancy was seen between two radiologists. In 13 patients with one MN, MN consisted of high-grade dysplasia in 10 patients and low-grade dysplasia in one patient, and fibrotic stroma between dilated branch ducts in two patients. In a patient with two MNs, both MNs consisted of high-grade dysplasia. Thus, MNs consisting of tumor cells were recognized in 12 (42.9%) of 28 patients on CE-MDCT and detected in the dilated branch ducts in 11 patients and in the MPD in one patient. Each of dilated pancreatic ducts (MPD and branch duct) judged as no associated MNs by two radiologists on CE-MDCT was pathologically lined by non-nodular low-height papillary epithelium in all patients. The mean diameter of the MNs on CE-MDCT was 9.2 mm ± 3.8 mm (standard deviation) (range 3.4–15.9) and not statistically significantly different from that (8.6.0 mm ± 3.6 mm [range 3.2–14.5]) ($p = 0.46$) on the pathologic specimens. Mean diameter of the MPDs was 8.5 ± 4.4 mm (range 3.4–21.0 mm) and not significantly different between patients with (9.3 ± 5.2 mm) and without (7.9 ± 3.8 mm) MN ($p = 0.35$). Mean diameter of the dilated branch ducts was 28.0 ± 18.5 mm (range 8.1–86.0 mm) and was not significantly different between patients with (30.6 ± 19.8 mm) and patients without (26.3 ± 18.5 mm) MNs ($p = 0.57$).

Qualitative evaluation of invasive components on CE-MDCT based on pathologic findings in patients with invasive IPMN

A 5-point scale assessment of the presence of the invasive component on CE-MDCT revealed excellent agreement between the two radiologists with weighted κ statistics of 0.87 (95% CI 0.73, 0.99) in the pancreatic parenchymal phase, 0.82 (95% CI 0.71, 0.94) in the portal venous phase, and 0.88 (95% CI 0.79, 0.97) in the equilibrium phase. Detectability rates of the invasive component in the pancreatic parenchymal phase were 85.7% and 82.1% for radiologists 1 and 2, respectively, and significantly higher than those in the portal venous and equilibrium phases in both radiologists. All of the invasive components were detected in the pancreatic parenchymal phase as hypoattenuating areas against a background of hyperattenuating pancreatic parenchyma by each radiologist (Table 2). Discrepancy over the presence of an invasive component was encountered in one patient in the pancreatic parenchymal phase. In four patients, an invasive component could not be detected in the pancreatic parenchymal phase by either radiologist. All of the invasive components detected by each radiologist on CE-MDCT were pathologically confirmed as tumor invasion. The mean diameter of the invasive components on the pathologic specimens in all 28 patients was 11.4 ± 10.7 mm (range 1.0–52.0 mm). The mean diameter of the detected and undetected invasive components on CE-MDCT was 13.0 ± 10.8 mm (range 3.7–52.0 mm) and 2.0 ± 0.8 mm (range 1.0–3.0 mm), respectively. The mean diameter of invasive components was not significantly different between patients with (11.8 ± 14.2 mm) and without (11.1 ± 7.6 mm) MNs ($p = 0.66$). The sites of origin of the invasive components were dilated MPD in eight patients, dilated branch duct in 16 patients, and both in four patients. Histologic types of the invasive components were 27 tubular adenocarcinomas and one mucinous adenocarcinoma. On histology, the invasive components contained more abundant fibrous stroma than the surrounding pancreatic parenchyma in all patients.

Table 2 Qualitative assessment of the invasive components on triple-phase CE-MDCT in two radiologists

	Radiologist 1			Radiologist 2		
	PPP	PVP	EP	PPP	PVP	EP
Detectable	24 (85.7)	11 (39.3)	11 (39.3)	23 (82.1)	11 (39.3)	12 (42.9)
Undetectable	4 (14.3)	17 (61.7)	17 (61.7)	5 (17.9)	17 (61.7)	16 (57.1)
Hypoattenuating area	24 (100)	11 (100)	9 (81.8)	23 (100)	11 (100)	10 (83.3)
Hyperattenuating area	0 (0)	0 (0)	2 (18.2)	0 (0)	0 (0)	2 (16.7)

Unless otherwise indicated, values are patients' number with percentages in parentheses. Detectability of the invasive components was significantly higher in the pancreatic parenchymal phase (PPP) than in the portal venous phase (PVP) ($p<0.001$ for radiologist 1 and $p=0.002$ for radiologist 2) and equilibrium phase (EP) ($p<0.001$ for radiologist 1 and $p=0.005$ for radiologist 2). There was no statistically significant difference between PVP and EP for each radiologist ($p=1.0$)

Relationships between MNs and the invasive components on the basis of CE-MDCT and pathologic findings

Continuity from high-grade dysplasia within the MN to the invasive component was confirmed on pathology in five (41.7%) of the 12 patients with MNs. In one patient with two MNs, only one MN was continuous with the invasive component. The mean diameter of the MNs was not significantly different between patients with (9.1 ± 4.0 mm) and without (10.0 ± 3.3 mm) continuity between MN and the invasive component ($p=0.67$). Both MNs and invasive components were detected by two radiologists on CE-MDCT in ten patients. For these ten patients, a 5-point scale assessment of the continuity between MN and invasive component on CE-MDCT revealed good agreement between the two radiologists with weighted κ statistics of 0.79 (95% CI 0.60, 0.98). The continuity was detected by each radiologist with no discrepancy on CE-MDCT in all five patients with pathologically proven continuity. Invasive IPMNs were classified into seven types on the basis of the relationships between MNs and invasive components in the pathologic findings in 28 patients (Fig. 1). In five patients with continuity between the MN and the invasive component, they were recognized in a dilated branch duct (Type I; $n=3$) (Fig. 2) and in the dilated MPD (Type II; $n=2$). In seven patients without continuity, all of the MNs were recognized in dilated branch ducts, and invasive components derived from the dilated branch ducts (Type III; $n=6$) (Fig. 3) and dilated MPDs (Type IV; $n=1$). In 16 patients without MNs, invasive components derived from dilated branch ducts (Type V; $n=7$) (Fig. 4), dilated MPDs (Type VI; $n=6$), and both (Type VII; $n=3$).

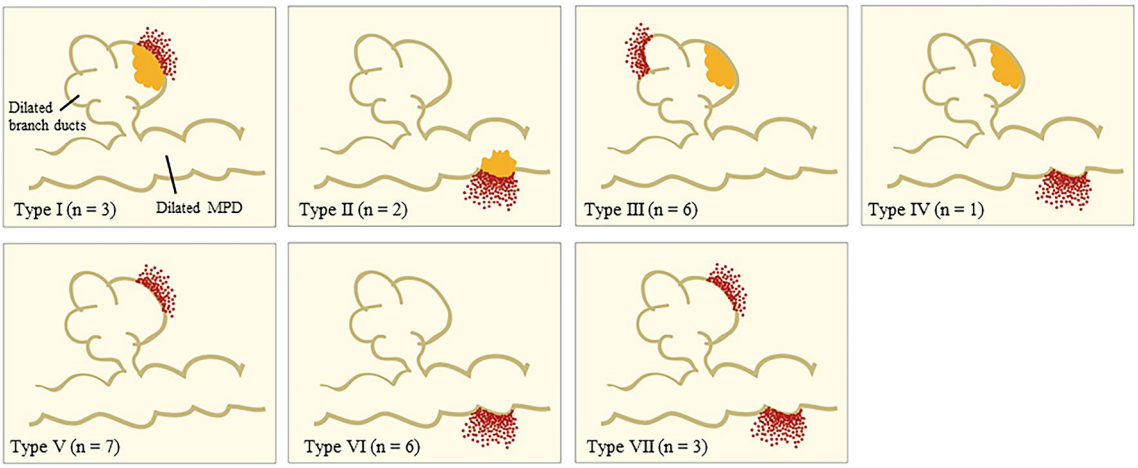

Fig. 1 Schematic illustration showing the morphological relationships between the mural nodules and invasive components on the basis of CE-MDCT and pathologic findings. Types I ($n=3$) and II ($n=2$) have a continuity between the mural nodule (MN) (yellow) and the invasive component (red dots) in the dilated branch duct and main pancreatic duct (MPD), respectively. Type III ($n=6$) has no continuity between the MN and the invasive component derived from a dilated branch duct. Type IV ($n=1$) has no continuity between the MN in a dilated branch duct and the invasive component derived from the dilated MPD. Type V ($n=7$), VI ($n=6$), and VII ($n=3$) have no mural nodule, and have invasive components derived from the dilated branch duct, dilated MPD, and both, respectively

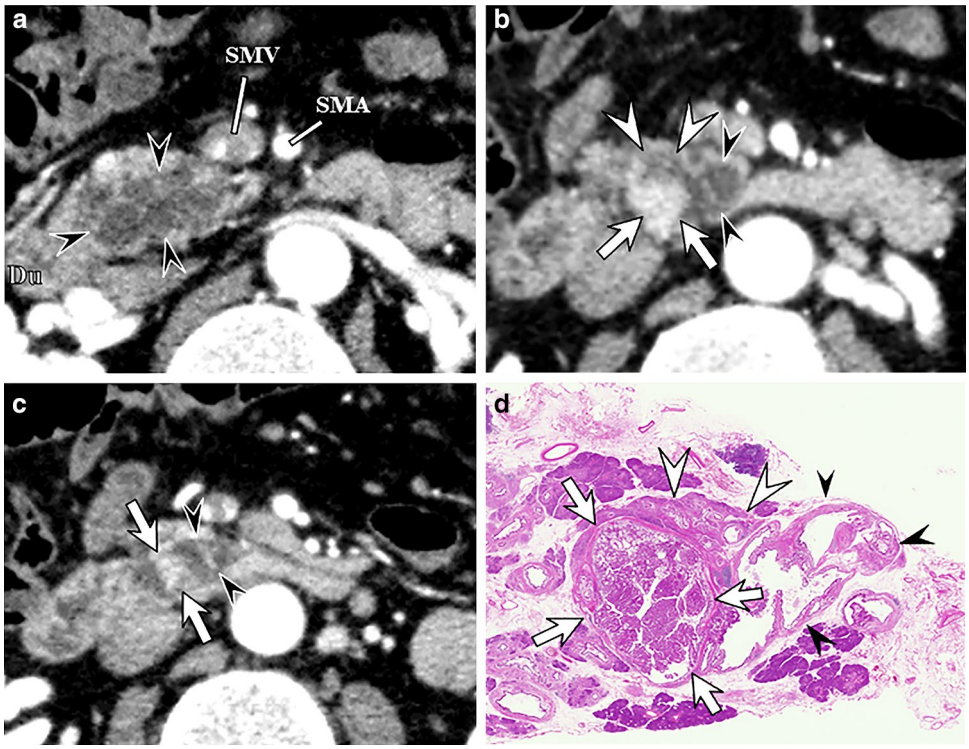

Fig. 2 Fifty-eight-year-old man with invasive intraductal papillary mucinous neoplasm (Type I). **a**–**c** Multiplanar reconstruction images in the pancreatic parenchymal phase perpendicular to the main pancreatic duct corresponding to the pathologic sections show the dilated branch ducts (black arrowheads in **a**–**c**) and enhancing mural nodule (MN) (arrows in **b** and **c**) in the pancreatic head. Hypoattenuating area (white arrowheads in **b**) contiguous with the enhancing MN is recognized. **d** Photomicrograph corresponding to the image **b** shows the dilated branch ducts (black arrowheads) and transition from the high-grade dysplasia within the MN (arrows) to the invasive component (white arrowheads) (haematoxylin–eosin stain; original magnification, ×4). The invasive component corresponds to the hypoattenuating area (white arrowheads in **b**). *SMA* superior mesenteric artery, *SMV* superior mesenteric vein, *Du* duodenum

Discussion

It has been reported that the presence of an enhancing MN is one of the important predictive factors for malignant behavior in IPMN and an important factor for determining its management [8, 11, 12] and enhancing MNs were recognized in 53.2% (33 of 62), 57.6% (34 of 59), and 67.3% (35 of 52) of the malignant IPMNs (high-grade dysplasia and invasive carcinoma) on CE-MDCT [9, 17, 20]. With regard to invasive IPMNs, previous studies have shown that MNs were recognized in 12 (57.1%) of 21 patients on EUS [25] and 28 (74%) of 38 patients on CE-MDCT [26]. In our study, enhancing MNs were detected on triple-phase CE-MDCT in 12 (42.9%) of 28 patients with invasive IPMN. The reason why the prevalence of MNs in patients with invasive IPMNs is lower than those of the above two reports may be due to our attention to only MNs exhibiting enhancement. From these results, careful attention should be paid to the existence of an invasive component even in the absence of an enhancing MN. Mean diameters of the dilated branch ducts, MPDs, and invasive components in patients with invasive IPMNs with MNs were not significantly different compared with those without MNs. In previous studies using triple-phase CE-CT, invasive components could be detected in 80−100% of patients with invasive IPMN [17, 20, 27] and most appeared as a hypoattenuating area in the pancreatic parenchymal phase [20, 27]. Similarly, in our study, the detectability of invasive components was significantly higher in the pancreatic parenchymal phase than that in the portal venous and equilibrium phases. All of the invasive components detected on CE-MDCT showed hypoattenuation in the pancreatic parenchymal phase. The reason for this is thought to be that the invasive components have abundant fibrous stroma, which reduces blood vessel density [27, 28]. It has been reported that enhancement of the tumor on the pancreatic parenchymal phase correlates negatively with the extent of fibrosis in invasive ductal carcinoma of the pancreas [28]. Thus, if the invasive components have sparsely distributed fibrotic stroma, these would be expected to show visible hyperattenuation in the pancreatic parenchymal phase. The diameters of the invasive components have not been previously assessed on imaging modalities including CT, MRI, and EUS in correlation with pathologic findings. In our study, pancreatic parenchymal phase

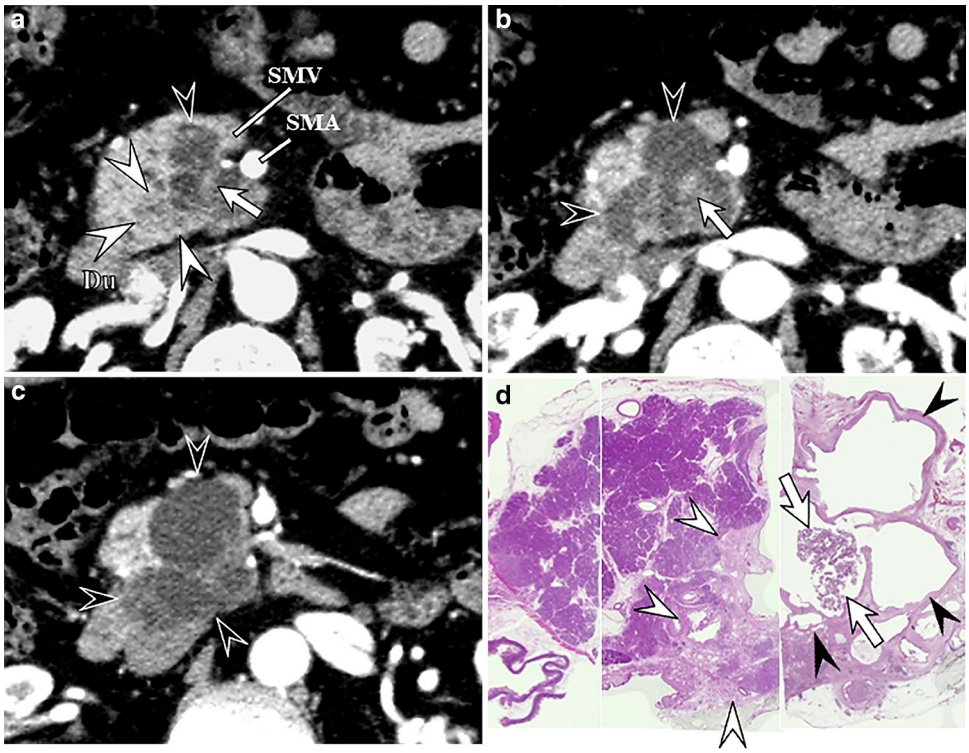

Fig. 3 Fifty-year-old man with invasive intraductal papillary mucinous neoplasm (Type III). **a**–**c** Multiplanar reconstruction images perpendicular to the main pancreatic duct corresponding to the pathologic sections in the pancreatic parenchymal phase show the dilated branch ducts (black arrowheads in **a**–**c**) and mural nodule (MN) (arrow in **a** and **b**) in the pancreatic head. Hypoattenuating area (white arrowheads in **a**) is recognized surrounding the dilated branch duct. **d** Photomicrograph corresponding to the image **a** shows the mural nodule (arrows) in the dilated branch duct (black arrowheads) and the invasive component (white arrowheads) derives from non-nodular low-height papillary epithelium with high-grade dysplasia (haematoxylin–eosin stain; original magnification, ×4). The invasive component corresponds to the hypoattenuating area (white arrowheads in **a**). *SMA* superior mesenteric artery, *SMV* superior mesenteric vein, *Du* duodenum

images allowed the detection of the invasive components of ≥ 3.7 mm in diameter and thus may be useful for early-stage diagnosis of invasive IPMN. As far as the site of origin of invasive components, branch ducts (57.1%) were more common than the MPD (28.6%) or both branch ducts and MPD (14.3%). To our knowledge, there have been no reports on the pathologic relationships between MNs and the invasive components in patients with invasive IPMN. From our results, invasive IPMN was classified into seven types based on the relationships between MNs and invasive components in the pathologic findings in 28 patients. Though we speculated that the invasive component derives from high-grade dysplasia within the MNs, invasive components contiguous with MNs were recognized in 5 (41.7%) of 12 patients with MN (Type I and II). When combined seven patients without the continuity between MNs and invasive components and 16 patients without MNs, the invasive component pathologically derived from non-nodular low-height papillary epithelium with high-grade dysplasia in 23 (82.1%) of all 28 patients (Type III−VII). It is important to assess the entire pancreatic parenchyma surrounding any dilated pancreatic ducts in the pancreatic parenchymal phase in order to identify invasive component irrespective of the presence or the absence of an MN.

There are several limitations to our study. First, there may have been an unavoidable selection bias because of its retrospective nature. Second, the patient number was relatively small and although it may have been enough to evaluate the MNs and invasive components on CE-MDCT on the basis of pathologic findings, larger-scale studies are needed to validate our present results. Third, our study was performed using MDCT. According to current guidelines, MRI is recommended for evaluation and follow-up of IPMN to avoid the ionizing radiation exposure associated with CT [8, 11, 12, 29]. It is speculated that similar results could be obtained using MRI, because MRI examination has shown similar diagnostic performance for IPMN compared with CT [15–17], but further study is needed. Fourth, our study included only patients with invasive IPMN. The radiologists were aware of the diagnosis of IPMN, but they were blinded to details regarding the pathologic findings (low-grade dysplasia, high-grade dysplasia, and invasive carcinoma).

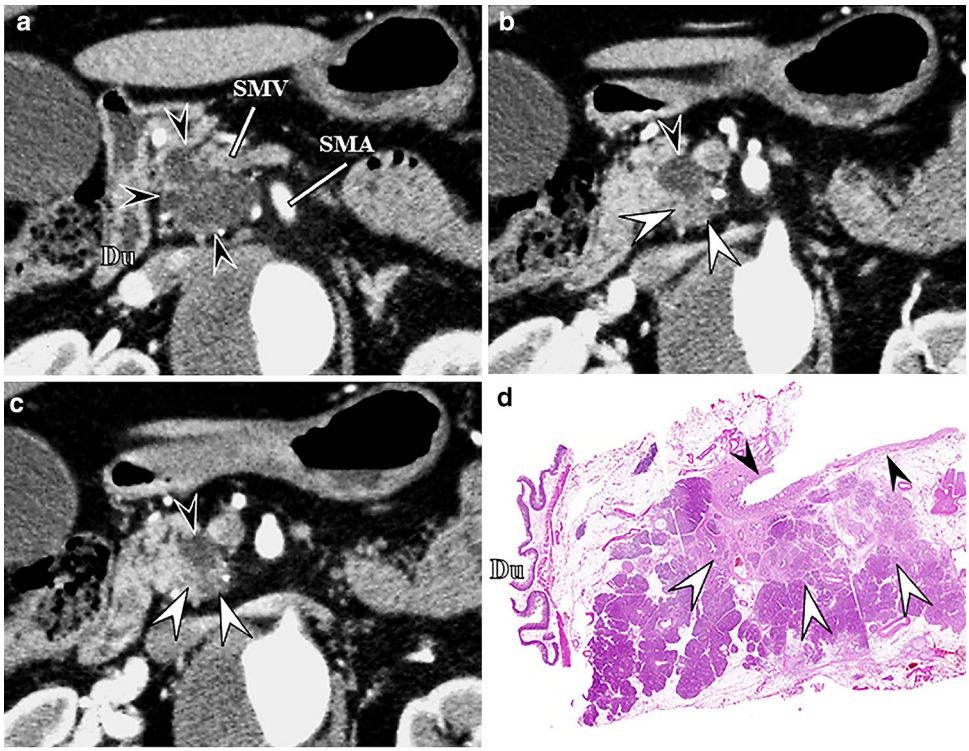

Fig. 4 Eighty-year-old man with invasive intraductal papillary mucinous neoplasm (Type V). **a**–**c** Multiplanar reconstruction images perpendicular to the main pancreatic duct corresponding to the pathologic sections in the pancreatic parenchymal phase show the dilated branch ducts (black arrowheads in **a**–**c**) in the pancreatic head. Hypoattenuating area (white arrowheads in **b** and **c**) is recognized surrounding the dilated branch duct. Mural nodule is not to be detected. **d** Photomicrograph corresponding to the image **b** shows the dilated branch ducts (black arrowheads) and the invasive component (white arrowheads) derives from non-nodular low-height papillary epithelium with high-grade dysplasia (haematoxylin–eosin stain; original magnification, ×4). The invasive component corresponds to the hypoattenuating area (white arrowheads in **b**). *SMA* superior mesenteric artery, *SMV* superior mesenteric vein, *Du* duodenum

In conclusion, the invasive components derived more often from low-height papillary epithelium without MN appearance on CE-MDCT than from MN. The pancreatic parenchymal phase on thin-section CE-MDCT may be the optimal phase for detection of small-invasive component.

References

1. Hruban RH, Takaori K, Klimstra DS et al. (2004) An illustrated consensus on the classification of pancreatic intraepithelial neoplasia and intraductal papillary mucinous neoplasms. Am J Surg Pathol 28:977-987.
2. Sohn TA, Yeo CJ, Cameron JL et al. (2004) Intraductal papillary mucinous neoplasms of the pancreas: an updated experience. Ann Surg 239:788-797.
3. Adsay, N.V., Fukushima, N, Furukawa, T. et al., Intraductal neoplasms of the pancreas. In: Bosman FT, Carneiro F, Hruban RH, Theise ND, editors. (2010) WHO classification of tumours of the digestive system: Lyon: WHO Press. pp 304-313.
4. Doi R, Fujimoto K, Wada M, Imamura M (2002) Surgical management of intraductal papillary mucinous tumor of the pancreas. Surgery 132:80-85.
5. Nara S, Shimada K, Kosuge T, Kanai Y, Hiraoka N (2008) Minimally invasive intraductal papillary-mucinous carcinoma of the pancreas: clinicopathologic study of 104 intraductal papillary-mucinous neoplasms. Am J Surg Pathol 32:243-255.
6. Kang MJ, Lee KB, Jang JY et al. (2013) Disease spectrum of intraductal papillary mucinous neoplasm with an associated invasive carcinoma: invasive IPMN versus pancreatic ductal adenocarcinoma-associated IPMN. Pancreas 42:1267-1274.
7. Tian X, Gao H, Ma Y, Zhuang Y, Yang Y (2015) Surgical treatment and prognosis of 96 cases of intraductal papillary mucinous neoplasms of the pancreas: a retrospective cohort study. Int J Surg 13:49-53.
8. Tanaka M, Fernández-del Castillo C, Adsay V et al. (2012) International Consensus Guidelines 2012 for the management of IPMN and MCN of the pancreas. Pancreatology 12:183-197.
9. Seo N, Byun JH, Kim JH et al. (2016) Validation of the 2012 International Consensus Guidelines using computed tomography and magnetic resonance imaging. Ann Surg 263:557-564.
10. Shimizu Y, Yamaue H, Maguchi H et al. (2013) Predictors of malignancy in intraductal papillary mucinous neoplasm of the pancreas: analysis of 310 pancreatic resection patients at multiple high-volume centers. Pancreas 42:883-888.
11. Tanaka M, Fernández-Del Castillo C, Kamisawa T, et al. (2017) Revisions of international consensus Fukuoka guidelines for the management of IPMN of the pancreas. Pancreatology 5:738-753.
12. European Study Group on Cystic Tumours of the Pancreas (2018) European evidence-based guidelines on pancreatic cystic neoplasms. Gut 67:789-804.

13. Kawada N, Uehara H, Nagata S, Tsuchishima M, Tsutsumi M, Tomita Y (2016) Mural nodule of 10 mm or larger as predictor of malignancy for intraductal papillary mucinous neoplasm of the pancreas: Pathologic and radiological evaluations. Pancreatology 16:441-448.
14. Pedrosa I, Boparai D (2010) Imaging considerations in intraductal papillary mucinous neoplasms of the pancreas. World J Gastrointest Surg 27:324-330.
15. Nakagawa A, Yamaguchi T, Ohtsuka M, et al. (2009) Usefulness of multidetector computed tomography for detecting protruding lesions in intraductal papillary mucinous neoplasm of the pancreas in comparison with single-detector computed tomography and endoscopic ultrasonography. Pancreas 38:131-136.
16. Choi SY, Kim JH, Yu MH, Eun HW, Lee HK, Han JK (2017) Diagnostic performance and imaging features for predicting the malignant potential of intraductal papillary mucinous neoplasm of the pancreas: a comparison of EUS, contrast-enhanced CT and MRI. Abdom Radiol (NY) 42:1449-1458.
17. Kang HJ, Lee JM, Joo I, et al. (2016) Assessment of Malignant Potential in Intraductal Papillary Mucinous Neoplasms of the Pancreas: Comparison between Multidetector CT and MR Imaging with MR Cholangiopancreatography. Radiology 279:128-139.
18. Vullierme MP, Giraud-Cohen M, Hammel P, et al. (2007) Malignant intraductal papillary mucinous neoplasm of the pancreas: in situ versus invasive carcinoma surgical resectability. Radiology 245:483-490.
19. Manfredi R, Graziani R, Motton M, et al. (2009) Main pancreatic duct intraductal papillary mucinous neoplasms: accuracy of MR imaging in differentiation between benign and malignant tumors compared with histopathologic analysis. Radiology 253:106-115.
20. Ogawa H, Itoh S, Ikeda M, Suzuki K, Naganawa S (2008) Intraductal papillary mucinous neoplasm of the pancreas: assessment of the likelihood of invasiveness with multisection CT. Radiology 248:876-886.
21. Yamada Y, Mori H, Matsumoto S, Kiyosue H, Hori Y, Hongo N (2010) Pancreatic adenocarcinoma versus chronic pancreatitis: differentiation with triple-phase helical CT. Abdom Imaging 35:163-171.
22. Furuhashi N, Suzuki K, Sakurai Y, Ikeda M, Kawai Y (2015) Naganawa S, Differentiation of focal-type autoimmune pancreatitis from pancreatic carcinoma: assessment by multiphase contrast-enhanced CT. Eur Radiol 25:1366-1374.
23. Tamada T, Ito K, Kanomata N et al. (2016) Pancreatic adenocarcinomas without secondary signs on multiphasic multidetector CT: association with clinical and histopathologic features. Eur Radiol 26:646-655.
24. Landis JR, Koch GG (1977) The measurement of observer agreement for categorical data. Biometrics 33:159-174.
25. Koshita S, Fujita N, Noda Y et al. (2015) Invasive carcinoma derived from "flat type" branch duct intraductal papillary mucinous neoplasms of the pancreas: impact of classification according to the height of mural nodule on endoscopic ultrasonography. J Hepatobiliary Pancreat Sci 22:301-309.
26. Kim JH, Eun HW, Kim KW et al. (2013) Intraductal papillary mucinous neoplasms with associated invasive carcinoma of the pancreas: imaging findings and diagnostic performance of MDCT for prediction of prognostic factors. AJR Am J Roentgenol 201:565-572.
27. Yamada Y, Mori H, Matsumoto S, Hijiya N, Hongo N, Moriyama M (2010) Invasive carcinomas originating from intraductal papillary mucinous neoplasms of the pancreas: conspicuity and primary sites of the solid masses on triple-phase dynamic CT imaging. Abdom Imaging 35:181-188.
28. Hattori YI, Gabata T, Matsui O et al. (2009) Enhancement patterns of pancreatic adenocarcinoma on conventional dynamic multi-detector row CT: correlation with angiogenesis and fibrosis. World J Gastroenterol 15:3114-3131.
29. Vege SS, Ziring B, Jain R, Moayyedi P (2015); Clinical Guidelines Committee; American Gastroenterology Association. American gastroenterological association institute guideline on the diagnosis and management of asymptomatic neoplastic pancreatic cysts. Gastroenterology 148:819-822.